Catalysis Today 138 (2008) 55–61

Contents lists available at ScienceDirect

Catalysis Today

journal homepage: www.elsevier.com/locate/cattod

Reactivity of perovskite-type precursor in MWCNTs synthesis

M. Kuras, Y. Zimmermann, C. Petit *

LMSPC-Laboratoire des Matériaux, Surfaces et Procédés pour la Catalyse, UMR 7515 du CNRS, ECPM, 25 rue Becquerel, 67087 Strasbourg Cédex 2, France

ARTICLE INFO

Article history:
Available online 16 June 2008

Keywords:
Nickel
Electronic microscopies
Perovskite
CVD
Diameter of carbon nanotubes

ABSTRACT

Ni catalysts were tested in the synthesis of multi-wall carbon nanotubes (MWCNTs) by catalytic decomposition of methane at low temperature. The selectivity of MWCNTs formation was determined using transmission electron microscopy (TEM). The catalytic performance of the supported-Ni catalysts obtained by perovskite reduction was discussed based on the X-ray diffraction (XRD), TEM and scanning electronic microscopy (SEM) results. The characteristics of the nanotubes obtained by decomposition of methane were mainly dependent on the homogeneity of nickel particles and less on the reaction conditions.

1. Introduction

In 1993, the catalytic approach for multi-wall carbon nanotubes (MWCNTs) formation was used for the first time by Yacaman et al. [1] and this method can be scaled up easily to industrial production. However, the carbon nanotubes formed by CVD-process, through the catalytic decomposition of carbon containing gas, have larger diameters and wide size distribution than those produced by the high temperature methods [2,3]. Nevertheless, the structure of the nanotubes formed in CVD-process is well crystallized and many works are actually focused on the production of aligned MWCNTs by CVD [4]. The catalytic decomposition of CH_4 is a sensitive reaction to the changes in the reactional procedure and allows obtaining the carbon nanotubes only when the catalyst is perfectly adapted, i.e. with a narrow metal particles size distribution [5].

The metal particles size seems to be the key parameter in the MWCNTs formation. The undertaken studies on carbon nanotubes production show the correlation between the tubes diameter and active nanoparticles size [6]. That is why it is very important to prepare the catalyst with homogeneous metal particles sizes. The nickel nanoparticles size is determined by the nucleation and the growth which strongly depend on the temperature [7,8] and nature of the reducing gases [9,10]. In the case of the perovskite $LaNiO_3$ which contains a reducible element (Ni^{III+}), the controlled reduction under H_2 led to the catalyst formation of Ni^0 metallic crystallites deposited on lanthanum oxide. The size of the formed crystallites during the reduction depends on the structure and texture of perovskite [11]. The selectivity and the yield of the reaction are closely related to the catalyst resistance to sintering in CVD-process.

On the other hand, the production of carbon nanotubes on the heterogeneous deposit in form of nanotubes and/or amorphous carbon mixture is related to the reactional conditions, i.e. temperature, time of the reaction but also to the selected carbon source [12]. The most frequently used sources of carbon for MWCNTs production are CH_4 [13,14], C_2H_2 [15], C_2H_4 [16,17], alcohols [18], and aromatics [19,20]. The temperatures for the MWCNTs synthesis by CVD under CH_4 are generally between 650 and 900 °C [21–23].

The aim of this paper is to present the study of the selectivity to MWCNTs formation on the unique phase of $LaNiO_3$ as a function of three parameters: temperature, time of reduction and CH_4/H_2 ratio.

2. Experimental

2.1. Preparation of the precursor

The perovskite is synthesized by the resin method from $Ni(OOCCH_3)_2{\cdot}4H_2O$ and La_2O_3 (Eq. (1) in solution and Eq. (2) during the calcination). The used solvent was propionic acid. A detailed description is presented in the previous publication [24].

* Corresponding author. Tel.: +33 3 90 24 27 69; fax: +33 3 90 24 27 68.
E-mail address: petitc@ecpm.u-strasbg.fr (C. Petit).

0920-5861/$ – see front matter © 2008 Elsevier B.V. All rights reserved.
doi:10.1016/j.cattod.2008.04.030

The perovskite structure is formed during the heat treatment at 900 °C of 4 h

$$La_2O_3 + 2Ni(OOCCH_3)_2{\cdot}4H_2O + 10CH_3CH_2COOH \rightarrow 2La(CH_3CH_2COO)_3 + 2Ni(CH_3CH_2COO)_2 + 7H_2O + 4CH_3COOH \quad (1)$$

$$2La(CH_3CH_2COO)_3 + 2Ni(CH_3CH_2COO)_2 + 35.5O_2 + \Delta \rightarrow 2LaNiO_3 + 30CO_2 + 25H_2O \quad (2)$$

2.2. Preparation of the Ni catalysts

The perovskite is reduced to give the catalysts. To ensure a total reduction of nickel included in $LaNiO_3$, we choose to carry out the reduction under hydrogen at the temperature close to 600 °C with a heating step under He of 15 °C/min and when the temperature is obtained the H_2 (2 ml/min) is introduced. This should allow the decreasing of the contact time of the perovskite structure with reducing gas in order to obtain small size nickel particles.

2.3. Description of the test conditions

When the perovskite is reduced, the CH_4 is added to the gas mixture. The H_2 flow is maintained during CVD-process to the same flux as for the reduction. The set-up is a standard fixed-bed continuous flow catalytic reactor.

Seven alternatives of operational protocol have been tested as presented in Table 1 in order to determine the catalyst effectiveness in the selective MWCNTs formation. According to the literature, the MWCNTs synthesis could be carried out under a gas mixture CH_4/H_2 with volume ratios from 3 to 20 [25–27]. Initially CH_4/H_2 ratio was equal to 1.5 and later was increased to 2.5 and 4.4. In the same way, the temperature and the time of reduction and reaction have been changed for the various tests.

The efficiency of the catalysts was reported in terms of methane conversions and percentage of carbon deposition. The percentage of carbon deposition is defined as follows:

$$\text{Carbon deposition}\,(\%) = 100 \times \frac{\text{weight of carbon deposed on the catalyst}}{\text{weight of Ni portion of the catalyst}}$$

The product gases were analyzed using an on-line gas mass spectrometer.

2.4. Techniques of characterization

- The Ni/La ratio for the perovskite was analyzed by elemental analysis, the distribution of particles by transmission electron microscopy (TOPCON EM-002B) and its texture by scanning electronic microscopy (SEM) (JEOL JMS 840). The adopted EDX method analysis [28], permits a global analyses of sample zones at about 200 nm and the local analyses at around 14 nm. These analyses when carried out in different places of the sample allow the verification of its homogeneity. For the solid $LaNiO_3$, the detected elements are O, Ni and La.
- The reduction of the perovskite is made under hydrogen. To quantify the amount of reducible nickel, we have followed the reducibility of the catalyst by temperature-programmed reduction (TPR) performed on 200 mg of catalyst placed in a U-shaped quartz tube (6.6 mm i.d.). The reductive gas mixture, H_2 (0.12 l h^{-1}) diluted in Ar (3 l h^{-1}), passes through the reactor which is heated from room temperature to 950 °C with a slope of 15 °C min^{-1} and then maintained at 950 °C until the end of H_2 consumption according to the baseline return. A thermal conductivity detector (TCD) was used for the quantitative determination of hydrogen consumption. After the TPR, the formed phases are controlled by X-ray diffraction (XRD).
- X-ray diffraction patterns of the perovskite and catalysts were measured by Bruker D-8 diffractometer, using Cu Kα radiation. Intensity was measured by step scanning in the 2θ range of 20–90° with a step of 0.02° and a step time of 2 s. The average Ni^0 size was obtained by the Scherrer equation based on the half-width of diffraction lines assigned to Ni (1 1 1).
- After each test, the crystallite size of nickel and the deposited carbons were analyzed by transmission electron microscopy (TEM).
- The quality of the obtained carbon nanotubes are quantified as well by the thermogravimetric analysis (TGA, SETARAM 92-12). The experiment consists in observation of the change of initial mass (approximately 5 mg), gain or loss, as a function of heating in oxidative atmosphere (synthetic air 10 ml min^{-1} + He 10 ml min^{-1}).

3. Results and discussion

3.1. Characterization of the precursor

XRD analysis (Fig. 1) shows that the synthesized solid is characterized only by one phase—the rhombohedric $LaNiO_3$ perovskite perfectly crystallized (JCPDS No. 01-079-2451). The average crystallite size of the perovskite, according to the Debye–Scherrer's equation [29] is equal to 18.5 nm.

The $LaNiO_3$ texture was analyzed by the scanning electronic microscopy (Fig. 2a and b). The texture is very homogeneous for the whole sample. The grains size is located between 50 and

Table 1
Operating conditions for the seven catalytic tests of $LaNiO_3$

Test	Operating conditions
First test	Reduction temperature H_2, 600 °C; reduction time H_2, 30 min; reaction temperature CH_4–H_2, 600 °C; reaction time CH_4-H_2, 20 min; CH_4/H_2 ratio = 1.5
Series 1 Rea 40	Reduction temperature H_2, 580 °C; reduction time H_2, 15 min; reaction temperature CH_4–H_2, 580 °C; reaction time CH_4–H_2, 40 min; CH_4/H_2 ratio = 1.5
Series 1 Rea 60	Reduction temperature H_2, 580 °C; reduction time H_2, 15 min; reaction temperature CH_4–H_2, 580 °C; reaction time CH_4–H_2, 60 min; CH_4/H_2 ratio = 1.5
Series 1 Rea 120	Reduction temperature H_2, 580 °C; reduction time H_2, 15 min; reaction temperature CH_4–H_2, 560 °C; reaction time CH_4–H_2, 120 min; CH_4/H_2 ratio = 1.5
Series 1 Rea 240	Reduction temperature H_2, 580 °C; reduction time H_2, 15 min; reaction temperature CH_4–H_2, 580 °C; reaction time CH_4–H_2, 240 min; CH_4/H_2 ratio = 1.5
Series 2 Ratio 2.5	Reduction temperature H_2, 580 °C; reduction time H_2, 15 min; reaction temperature CH_4–H_2, 580 °C; reaction time CH_4–H_2, 120 min; CH_4/H_2 ratio = 2.5
Series 2 Ratio 4.4	Reduction temperature H_2, 580 °C; reduction time H_2, 15 min; reaction temperature CH_4–H_2, 580 °C; reaction time CH_4–H_2, 40 min; CH_4/H_2 ratio = 4.4

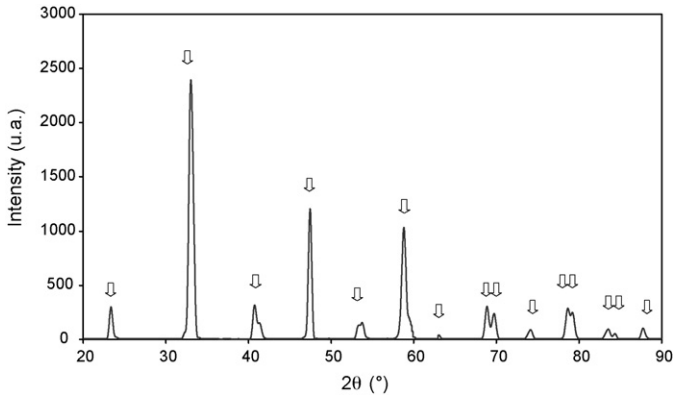

Fig. 1. XRD of $LaNiO_3$ treated at 900 °C. (⇩) $LaNiO_3$ rhombohedric.

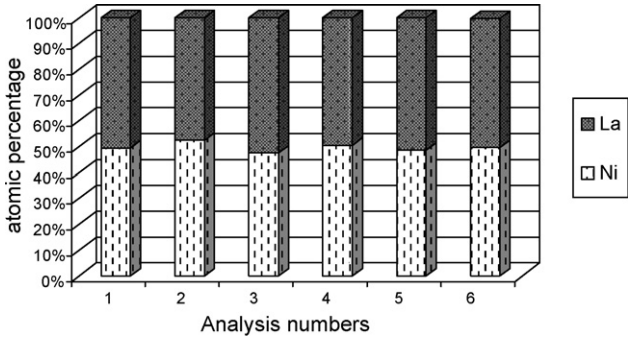

Fig. 3. EDX analysis, distribution of Ni and La atoms in $LaNiO_3$ after treatment at 900 °C. No. 1, global analysis zone of 200 nm; the other local analyses zones of 14 nm.

150 nm. It seems that three to seven diffracting crystallites of 18 nm are forming a particle. The BET of this sample is lower than 5 $m^2\ g^{-1}$ which favors the aggregation of particles.

According to the atomic adsorption, the La/Ni ratio is equal to 1. An analysis of lanthanum and nickel atoms distribution was verified on nanometric scale by X-ray spectroscopy with dispersion of energy (EDX) coupled with the high-resolution transmission microscope. No matter the zones global or local the La/Ni atomic ratio is constant which proves the high homogeneity on nanometric level (Fig. 3). The difference in the values for the both analyses does not exceed 1.5–2.5% and can be concluded that the obtained samples posses a very homogeneous structure.

3.2. Reduction of the precursor

H_2-TPR analysis confirms the existence of only one oxidation state of nickel in the perovskite structure—Ni^{III+} (Fig. 4) [24].

The XR diffractograms of the samples made after the partial reduction of the perovskite (first peak in TPR) and after the complete reduction (second peak) confirm the formation of the phases: $La_2Ni_2O_5$ and Ni and La_2O_3, respectively. The two peaks correspond to the reduction of Ni^{III+} to Ni^{II+} and then of Ni^{II+} to Ni^0. After reduction the nickel nanoparticles deposited on La_2O_3 represents the active phase of the catalyst for MWCNTs production. The metal crystallites diameter obtained after H_2-TPR and calculated by the Scherrer–Debye's equation was estimated to 12 nm. This size represents the average of all diameters observed for the reduced nickel particles formed under H_2 reduction. The TEM analysis after H_2-TPR shows clearly the dispersion of the metal particles and its size after the reduction reaction (figure not presented). In fact, the sizes of nickel particles are various; the largest and less abundant particles have a diameter close to 33 nm. The most important part of reduced nickel particles adopts a size of approximately 16 nm. The last group of particles is formed by the entities smaller than 8 nm. The TEM data confirms the values calculated by the average diameter obtained by XRD.

One can conclude that the $LaNiO_3$ calcined at 900 °C has perfect crystallinity and the composition is homogeneous as well in the macroscopic as in microscopic scale.

3.3. Description of CVD-CH_4 tests

The first test was carried out entirely at 600 °C—to have the full reduction of perovskite precursor to Ni for 30 min of reduction. Then in order to control the nickel crystallite size the temperature of reduction as well as the temperature of the reaction was decreased. For all further tests the time of reduction under H_2 was shortened to 15 min and reaction temperature of 560 °C. According to Cui et al. [30] this temperature is sufficient for CH_4 activation.

Two series of tests are made, the increase of the reaction time from 40 through 120 to 240 min and on the other hand, the increase in CH_4/H_2 volume ratio from 1.5 through 2.5 to 4.4. This increase theoretically will keep the high yield of tubes despite of the increasing the time of reaction. With the increase of CH_4 flow,

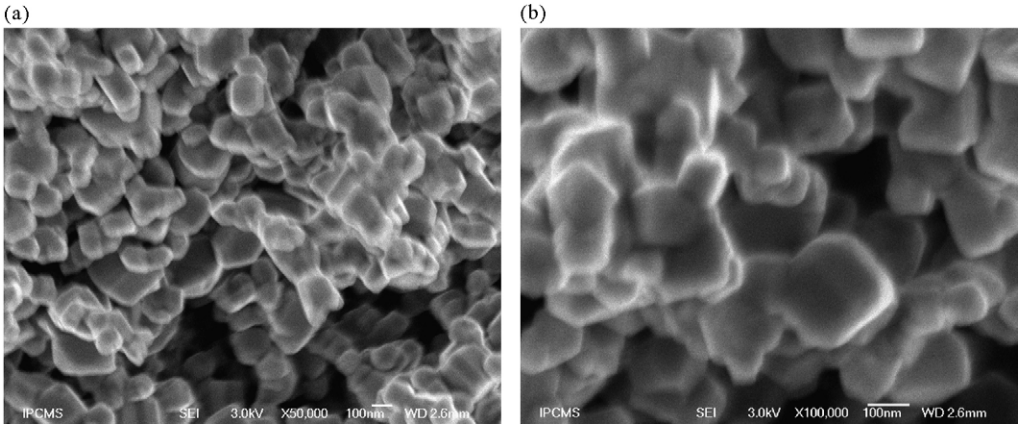

Fig. 2. SEM images of $LaNiO_3$ treated at 900 °C: (a) with an enlargement of 50.000 in mode SEI and (b) with an enlargement of 100.000 in mode SEI.

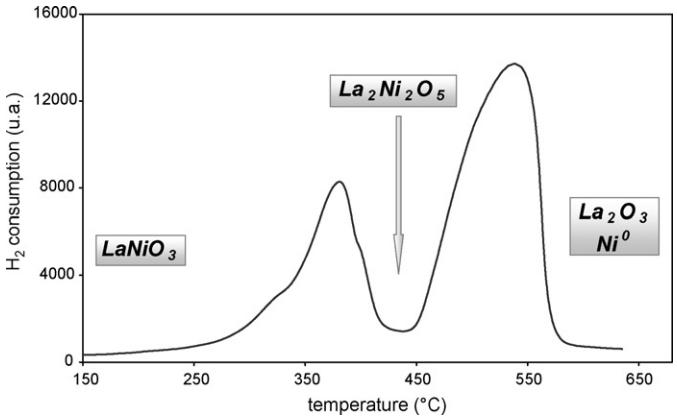

Fig. 4. H_2-TPR profile of $LaNiO_3$ treated at 900 °C.

the He flow was decreased in order to preserve the same total gas flow, at 40 ml/min.

3.4. Characterizations of deposited carbons

All the samples were analyzed post-MWCNTs synthesis by XRD, TEM and SEM. TEM images (Fig. 5) confirm that the majority of the carbonaceous deposit formed during the reaction was constituted by nanotubes. The observation of the images indicates that the amorphous carbon is present also but constitutes a small part of the carbonaceous deposit.

According to Pérez-Cabero et al. [31], the term "carbon nanotubes" is referring to the filamentous carbons with a center channel or a hollow core. In this paper, we adopted the definitions and confirm the MWCNTs formation. The external and internal diameters of MWCNTs were measured by means of TEM images (Fig. 5) and their lengths were estimated by means of SEM images in the areas with low density of tubes (Fig. 6). The distribution of the tubes as a function of their external and internal diameters is given in Table 2.

Table 2
Characterizations of the main distribution of MWCNTs obtained on $LaNiO_3$ treated at 900 °C after the CVD tests

Test	Internal tubes diameter (nm)	Thickness of walls (nm)
First test	6	1–4.5
Series 1 Rea 40	5.5–6	1–4.75
Series 1 Rea 60	5.5–6	2.25–4.5
Series 1 Rea 120	5.5–6	2.25–4.5
Series 1 Rea 240	6	2–4.5
Series 2 Ratio 2.5	3–5.5	1.25–6
Series 2 Ratio 4.4	5.5–6	2.25–4.5

The size of nickel crystallites obtained during the tests seems to depend only on the structure of the precursor. In all operating conditions, the metal particles size given by XRD varies between 13 and 14 nm. Neither the decrease in the temperature (600, 580 or 560 °C), nor the changes on the reduction time (30–15 min) or the reaction time (from 20 to 240 min) influences the size of Ni particles. The same is observed after the modifications of CH_4/H_2 volume ratio (from 1.5 to 4.4), which indicates that the metal particles size is primary related to the reduction step. To explain that no nickel sintering is visible, we proposed that the formation of tubes embryos is very fast and its presence limits the contact on the nickel particles staying the size obtained after the reduction under H_2. This is the case for all the tests made except for the ratio CH_4/H_2 equal to 4.4.

The carbon nanotubes diameter distribution can be directly related to the nickel particles size [32]. The calculation of Ni^0 particles size by XRD is precise only if the distribution of sizes is narrow. Only the transmission electron microscopy makes possible to establish the exact profile of particle size. However, when the

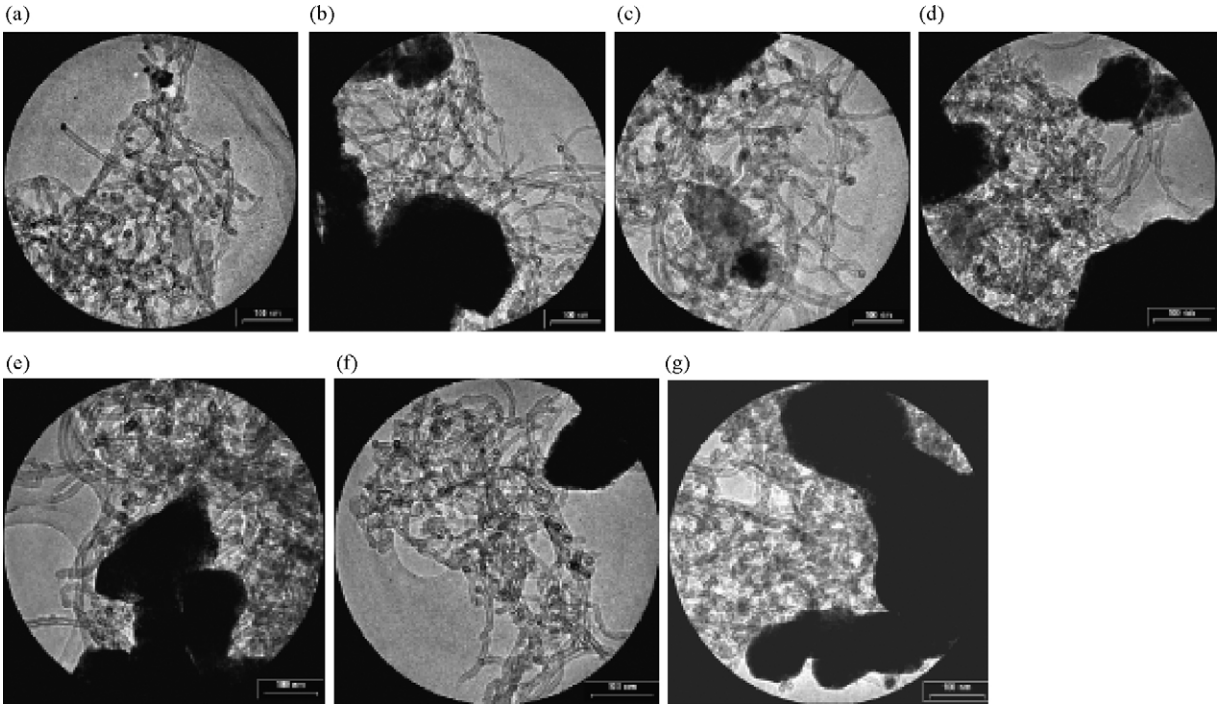

Fig. 5. TEM of $LaNiO_3$ treated at 900 °C with an enlargement of 20.000: (a) after first test; (b) after series 1 rea 40; (c) after series 1 rea 60; (d) after series 1 rea 120; (e) after series 1 rea 240; (f) after series 2 ratio 2.5; (g) after series 2 ratio 4.4.

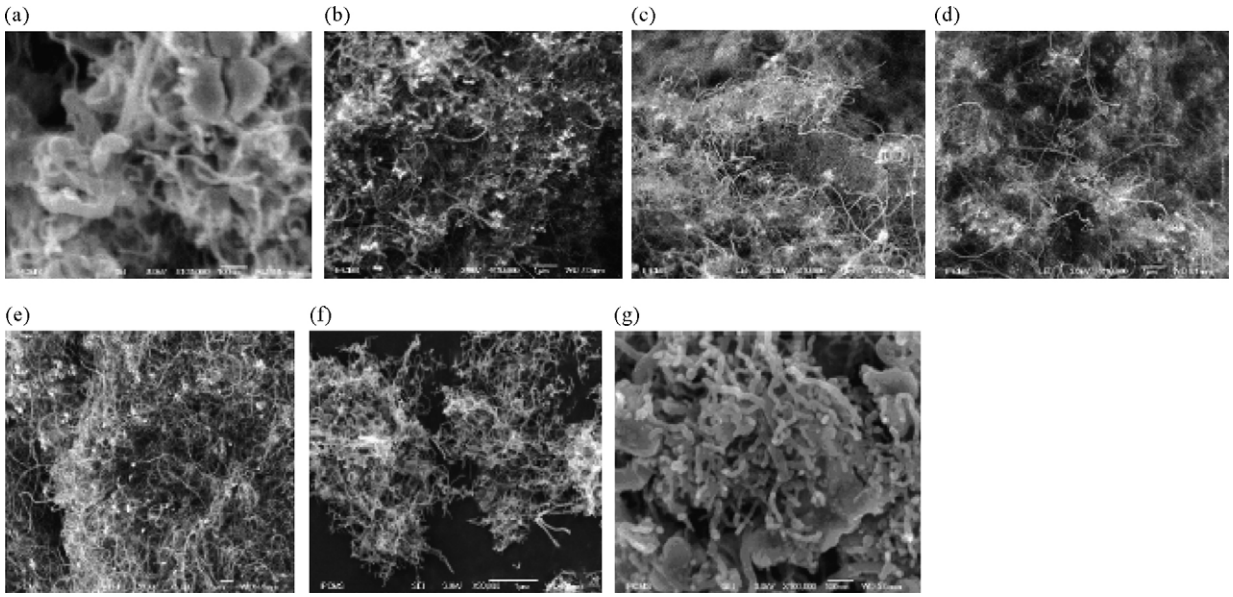

Fig. 6. TEM of $LaNiO_3$ treated at 900 °C in mode SEI: (a) after first test with an enlargement of 100.000; (b) after series 1 rea 40(10.000); (c) after series 1 rea 60 (10.000); (d) after series 1 rea 120 (10.000); (e) after series 1 rea 240; (f) after series 2 ratio 2.5 (5.000); (g) after series 2 ratio 4.4 with an enlargement of (100.000).

nanotubes are present on the surface, the nickel particles are not visible on TEM micrographs and it is the tubes diameter which could allow the confirmation of the average nickel particles size. The TEM profiles of the tubes for all different tests are presented in Fig. 7 and can be used for calculation of the nickel particle size.

For the reactions carried out with different volume ratios CH_4/H_2 of 1.5 and 2.5 the nickel particles size distributions are constant. The average size of 13 nm given by XRD seems to be justified very well with the majority of particles measured from all the tests at around 10–15 nm. It changes significantly for CH_4/H_2 volume ratio of 4.4 and two groups of nanotubes sizes were observed. The first characterized by average nanotubes diameter between 8 and 15 nm and the second group with larger diameter (16–30 nm, not presented in Table 2). The TEM profile describes better than XRD the influence of CH_4/H_2 ratio on the particles size (Fig. 7, no. 7). The decrease of the reduction time during CVD-process minimizes the sintering of the metal particles and leads to very narrow distribution (8–15 nm). The same result was obtained for the tests with 15 min reduction time and 40 min methane decomposition (Fig. 7, no. 2). The longer reaction time when duration of the reduction is the same leads to the weak sintering of nickel particles and indicate that the formation of the nanosized Ni particles is strongly related to the reduction of the perovskite under H_2. When CH_4/H_2 ratio remains inferior or equal to 2.5 the perovskite generates the Ni^0 particles with the same size. One could note the strong evolution in favour to the creation of larger aggregates during the test with CH_4/H_2 ratio equal to 4.4. This difference is not connected to the reduction step which does not change. The particles sintering thus takes place during the reaction of decomposition of methane. Just after the reduction, the size distribution must be close to one of the shorter test distribution presented in Fig. 7, no. 2 (40 min reaction). Some Ni^0 crystallites (50%) keep their initial size from approximately 8 to 15 nm. Other group of particles (48%) forms aggregates rather important in sizes (16–30 nm) according to the way presented in Fig. 8. In this case, the metal phase sintering occurs before the appearance of the tubes embryos and leads to the aggregation of several nickel particles resulting in thicker carbon nanotubes thereafter.

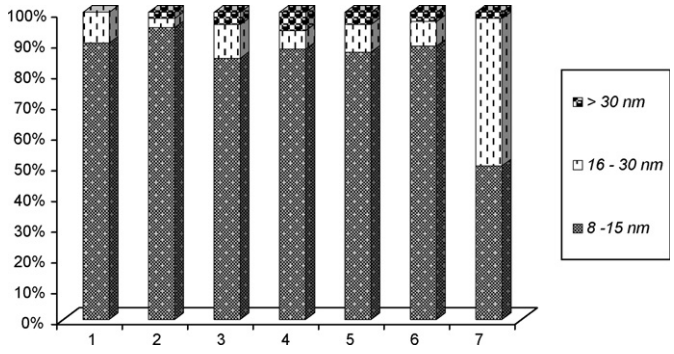

Fig. 7. Distribution of Ni^0 size after catalytic tests on $LaNiO_3$ according to the TEM results.

However, independently of the test time and CH_4/H_2 volume ratio inferior or equal to 2.5, the C_α rate of carbon diffusion through the metal particles and its precipitation thereafter are sufficiently fast so that the "nanoparticle - nanotube" assemblies formed in the nucleation step can isolate the nickel particles by carbon nanotube what prevents sintering of metallic nickel. This way one could claim that the fast nucleation is benefit to keep the small size of Ni^0 obtained during the reduction under H_2.

It was already reported that CH_4 decomposition depends on the degree of crystallization, the crystallite size and the morphology of the metal particles [33]. A reduction of the activity according to the increasing diameter during the test was already observed by other authors [34]. So, there exists an optimal size of the active phase particles for the CH_4 decomposition and for the formation of tubes. The different nickel particles sizes could result in various crystallized carbon forms. For the formation of carbon nanofibres the optimal size varies from 10 to 60 nm [35], 30 to 70 nm [36] or 34 nm [37] according to the operating conditions. In our case the optimal size of nickel crystallites for carbon nanotubes under the proposed operating conditions lies between 10 and 15 nm. This interval of metal crystallites size leads to the highest carbon nanotubes yield. In fact, whatever the operating conditions are the carbon nanotubes distribution is similar with an external diameter for the majority of approximately 10–15 nm.

However, few nickel particles of very important size (100 nm) are present. They are not considered in the size distributions

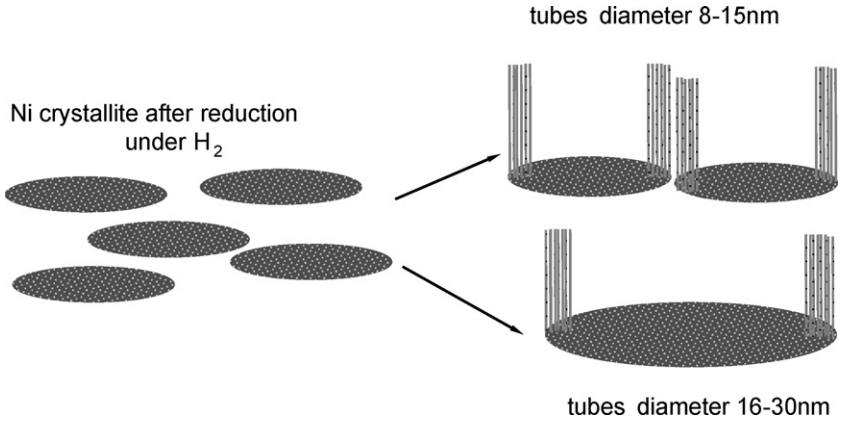

Fig. 8. Model of nickel particles recombination under the influence of the CH_4.

because of their marginal quantity. These large particles are not able to produce carbon nanotubes and they are not active in CH_4 decomposition. In fact, the activation energy for CH_4 catalytic decomposition increases with the Ni^0 particles size [35]. The big particles lead only to partial decomposition of methane which produces different carbonaceous species CH_3^{*-}, CH_2^{*2-}, CH^{*3-}. These carbons containing fragments react one to another resulting in amorphous carbon deposition.

The prolongation of the reaction time had a significant influence on carbon nanotubes yield as presented in Table 3.

When the time of the synthesis increases from 60 min at 600 °C to 240 min test at lower temperature of 560 °C the yield increases twice. In the same way, the increase of CH_4/H_2 volume ratio and reduction of the reaction time also results in a good yield but the obtained carbon nanotubes are less structured.

The quality of the obtained carbon nanotubes obtained after test series 2 ratio 2.5, are tested as well by the thermogravimetric analysis (TGA) as presented in Fig. 9.

The total mass loss of this sample is about 3 mg. Initially, between the temperatures of 75 and 305 °C, two light gain of mass were observed. It is related to the nickel oxidation in NiO. In the high temperature zone (from 400 to 740 °C) an important loss of mass is visible. These temperatures correspond to the structured carbon combustion. The curve of the mass loss is not homogeneous; a weak break of the slope is visible between 670 and 740 °C. This change was not related to the combustion of different carbonaceous phases but to the slow oxygen diffusion which postpones the oxidation of all carbon species at the same time. This is rather expected if we take into account the important density of the carbonaceous deposit seen by SEM analysis. The XRD analysis confirms that after thermogravimetric analysis, a pure structure of initial perovskite was received, phenomenon already mentioned in the literature [38].

Taking into consideration the reactions series 1 rea 240 (CH_4/H_2 ratio equal to 1.5 and 240 min test duration) and series 2 ratio 2.5 (CH_4/H_2 ratio equal to 2.5 and 120 min duration) which have respectively the same yield of carbon nanotubes −35% and 37%. One can realize that for the same quantity of methane (total quantity of CH_4 at around 3×10^{-2} mol) supplied in shorter time, the carbon nanotubes yield remains constant.

The increase of the yield for the series of tests with a CH_4/H_2 ratio 1.5 is primarily related to the formation of longer tubes contrary to the yield of the CVD-process with the CH_4/H_2 ratio of 2.5 or 4.4 which is not connected with the length of the tubes but with their quantity. In fact, for these tests the length of the tubes decreases drastically but the quantity of the tubes embryos increases (Table 3).

The reaction time and the volume ratio of CH_4 and H_2 in the mixture influence the length of the carbon nanotubes. For a CH_4/H_2 ratio of 1.5 the length of the tubes increases with the reaction time and reaches 20 μm in 240 min reaction compared to 500 nm for the shorter tests. This indicates that the limiting step in the formation of carbon nanotubes is related to the appearance of the tubes embryos—nucleation, thus the formation of new tubes seems to be slower than the incorporation of carbon in already existing ones.

The mechanism of growth which we are going to adopt to explain the formation of carbon nanotubes under imposed conditions is that of "root" or "bases-growth" [39]. However, the increase of the CH_4 concentration led to the appearance of a small quantity of tubes which can be characterized by a growth close to "bamboo" [40,41] under CH_4 and H_2 (Fig. 10).

Table 3
Characterization of MWCNTs obtained on $LaNiO_3$ treated at 900 °C after the CVD tests, carbon yield of the catalytic tests and average length of tubes given by analysis SEM

Test	Carbon yield of the catalytic tests (%)	Average length of tubes
First test	–	300–500 nm
Series 1 Rea 40	–	3–7 μm
Series 1 Rea 60	5	7–10 μm
Series 1 Rea 120	11	10–15 μm
Series 1 Rea 240	35	15–20 μm
Series 2 Ratio 2.5	37	0.5–2 μm
Series 2 Ratio 4.4	–	300–400 nm

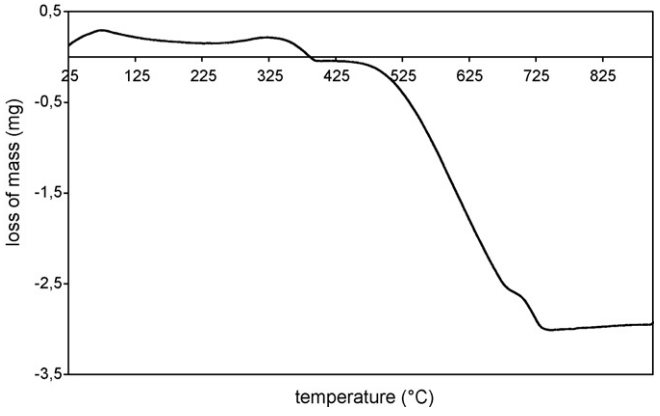

Fig. 9. TGA analysis after series 2 ratio 2.5.

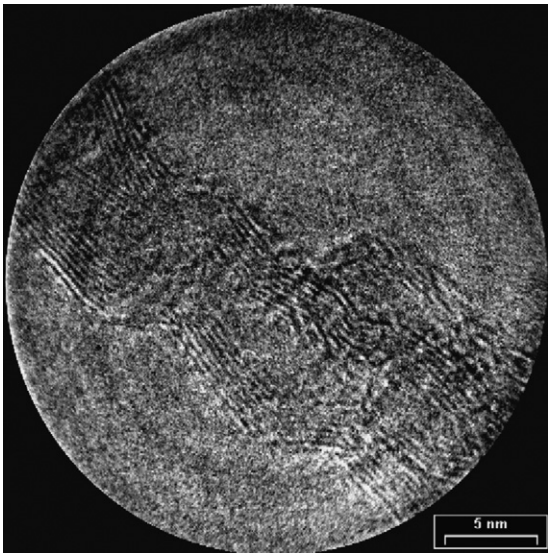

Fig. 10. HR-TEM of $LaNiO_3$ treated at 900 °C with an enlargement of 39.000 in mode SEI after series 2 ratio 2.5.

4. Conclusions

The obtained catalysts from the perovskite precursors are very resistant in time on stream and at high temperatures CVD. The changes of the temperature of the reduction do not influence the average size of the formed particles, which remain always close to 13 nm. Neither the reaction temperature nor the different CH_4/H_2 ratio had impact on the nickel nanoparticles size which led to the very similar carbonaceous deposit for all catalytic tests.

The modifications of the operating conditions applied to perovskite structure—$LaNiO_3$, namely, the reduction time under H_2, reaction time under CH_4–H_2 mixture, reduction temperature and/or the reaction temperature as well as CH_4/H_2 ratio did not disturb significantly the quality of the carbon nanotubes. Their principal characteristics remain intact. The distribution of nanotubes of this catalyst is always very homogeneous. The reaction yield increases with increase of the reaction time without influence on the quality of carbon nanotubes.

Acknowledgements

The authors would like to thank the GDRE 2756 for scientific organization. They are indebted to Dr. S. Ivanova for proof reading the manuscript.

References

[1] M.J. Yacaman, M.M. Yoshida, L. Rendon, J.G. Santiesteban, Appl. Phys. Lett. 62 (1993) 202.
[2] S. Iijima, Nature 354 (1991) 56.
[3] B. Zheng, C. Lu, G. Gu, A. Makarovski, G. Finkelstein, J. Liu, Nano Lett. 2 (2002) 895.
[4] W. Kim, H. Choi, H. Shim, M. Li, D. Wang, H. Dai, Nano Lett. 2 (2002) 703.
[5] G.A.L. Jablonski, F.W. Geurts, A. Sacco, R.R. Biederman, Carbon 30 (1992) 87.
[6] H. Dai, P. Nikolaev, A. Thess, A.G. Rinzler, D.T. Colbert, R.E. Smalley, Chem. Phys. Lett. 260 (1996) 471.
[7] J. Cosyns, in fundamental and industrial aspects of catalysis by metals, B. Imelik, G.A. Martin and A.J. Renouprez (eds), CNRS, Paris, 371.
[8] J.L. Katz, Pure Appl. Chem. 64 (1992) 1661.
[9] M.P. Moody, P. Attard, J. Chem. Phys. 117 (2002) 6705.
[10] R. Becker, W. Doring, Ann. Phys. (Berlin, Germany) 24 (1935) 719.
[11] J.T. Richardson, R. Scates, M.W. Twigg, Appl. Catal. 246 (2003) 137.
[12] G.A.L. Jablonski, F.W. Geurts, A. Sacco, Carbon 30 (1992) 99.
[13] Z. Jin, X. Li, W. Zhou, Z. Han, Y. Zhang, Y. Li, Chem. Phys. Lett. 432 (1–3) (2006) 177.
[14] Y.J. Yoon, J.C. Bae, H.K. Baik, S.J. Cho, S.J. Lee, K.M. Song, N.S. Myung, Phys. B: Conden. Mater. 323 (1–4) (2002) 318.
[15] G.P. Veronese, R. Rizzoli, R. Angelucci, M. Cuffiani, L. Malferrari, A. Montanari, F. Odorici, Physica E 37 (1/2) (2007) 21.
[16] N. Sano, M. Nobuzawa, Diamond Relat. Mater. 16 (2007) 144.
[17] J. Cheng, X. Zhang, Z. Luo, F. Liu, W. Yin, W. Liu, Y. Han, Mater. Chem. Phys. 95 (2006) 5.
[18] N. Inami, M. Mohamed, E. Shikoh, A. Fujiwara, Sci. Technol. Adv. Mater. 8 (2007) 292.
[19] K. Saeed, S.Y. Park, H.J. Lee, J.B. Baek, W.S. Huh, Polymer 47 (2006) 8019.
[20] B. Pawelec, V. La Parola, R. Navarro, S. Mascarós, J.G. Fierro, Carbon 44 (2006) 84.
[21] Z.F. Ren, Z. Huang, Z. Xu, J. Wang, P. Bush, M. Siegel, P.N. Provencio, Science 282 (1998) 1105.
[22] Z.F. Ren, Z. Huang, Z. Xu, J. Wang, Z. Wen, L. Calvet, E. Chen, J. Klemic, M. Reed, Appl. Phys. Lett. 75 (8) (1999) 1086.
[23] Y. Yudasaka, Z. Masoko, D. Rie, W. Matuie, K. Takeo, G. Yoshimasa, J. Kikuchi, X. Etsuro, Appl. Phys. Lett. 70 (14) (1997) 1817.
[24] M. Kuras, R. Roucou, C. Petit, J. Mol. Cat. A: Chem. 265 (2007) 210.
[25] Y.S. Woo, D.Y. Jeon, I.T. Han, N.S. Lee, J. Jung, J.M. Kim, Diamond Relat. Mater. 11 (2002) 59.
[26] W.Y. Lee, C.H. Weng, Z.Y. Juang, J.F. Lai, K. Leou, C.H. Tsai, Diamond Relat. Mater. 14 (11/12) (2005) 1852.
[27] T. Dikonimos Macris, L. Giorgi, R. Giorgi, N. Lisi, E. Salernitano, Diamond Relat. Mater. 14 (3–7) (2005) 815.
[28] M. Houalla, F. Delannay, I. Matsuura, B. Delmon, J. Chem. Soc. Faraday Trans. 76 (1980) 379.
[29] B.D. Cullity, Elements of X-ray diffraction, Wesley Publishing Company Inc., 1956
[30] Y. Cui, H. Xu, Q. Ge, Y. Wang, S. Hou, W. Li, J. Mol. Catal. A 249 (2006) 53.
[31] M. Pérez-Cabero, I. Rodríguez-Ramos, A. Guerrero-Ruíz, J. Catal. 215 (2003) 305.
[32] Z. Li, J. Chen, X. Zhang, Y. Li, K.K. Fung, Carbon 40 (2002) 409.
[33] J.J. Carberry, Catal. J. 114 (1998) 277.
[34] Boudart, J. Mol. Catal. 30 (1985) 27.
[35] P. Wang, E. Tanabe, K. Ito, J. Jia, H. Morioka, T. Shishido, K. Takehira, Appl. Catal. A 231 (2002) 35.
[36] T.V. Reshetenko, L.B. Avdeeva, R.Z. Ismagilov, A.L. Chuvilin, Carbon 42 (2004) 143.
[37] D. Chen, K.O. Christensen, E. Ochoa-Fernandez, Z. Yu, B. Totdal, N. Latorre, A. Monzon, A. Holmen, J. Catal. 229 (2005) 82.
[38] H. Provendier, Thesis, U.L.P. Strasbourg (France), 1998.
[39] L. Owens, J.M. McNeil, L.E. Liu, J. Am. Chem. Soc. 124 (2002) 13688.
[40] D.C. Li, L. Dai, S. Huang, A. Mau, Z.L. Wang, Chem. Phys. Lett. 316 (2000) 349.
[41] X. Wang, W. Hu, Y. Liu, C. Long, Y. Xu, S. Zhou, D. Zhu, L. Dai, Carbone 39 (2001) 1533.